Study of Nonstoichiometry and Physical Properties of the $Nd_{1-x}(Ba_{0.40}Mg_{0.60})_{1+x}FeO_{4-y}$ System

Chul Hyun Yo*, Kwon Sun Roh, and Soon Ho Chang†

Department of Chemistry, Yonsei University, Seoul 120-749, Korea
†Electronics and Telecommunications Research Institute, Taejon 305-606, Korea
Received December 1, 1994

A series of samples of the $Nd_{1-x}(Ba_{0.40}Mg_{0.60})_{1+x}FeO_{4-y}$($x$=0.00, 0.10, 0.20, and 0.30) system has been synthesized at 1450 ℃ under an atmospheric air pressure. The x-ray powder diffraction analysis of the solid solutions assigns the structure of all the compositions to orthorhombic system. Mohr salt analysis shows that τ and y values increase with x value and nonstoichiometric chemical formulas of the system can be formulated from the x, τ, and y values. Oxygen vacancies are distributed along c-axis in the perovskite layer. The magnetic ordering temperature remains unchanged with x value. Electrical conductivity and activation energy depend only on the mixed valence state of Fe ion. Conduction mechanism can be suggested as the hopping of electron between e_g orbitals of Fe^{3+} and Fe^{4+} ions through Fe^{3+}-O-Fe^{4+} bonds. Magnetic susceptibility and electrical conductivity are discussed with the nonstoichiometric chemical formulas.

Introduction

The K_2NiF_4-type oxides represented by $AO(ABO_3)$ or A_2BO_4 have four modified phases[1,2] such as tetragonal(T), orthorhombic(T), T′, and T* phases. The tetragonal phase has the ideal K_2NiF_4 structure. If the A-O bond length is small relative to the B-O one, the orthorhombic distortion occurs and T′ and T* phases are formed in the larger discrepancy between the A-O and B-O bond lengths. The ideal K_2NiF_4 structure is consisted of alternating layers of rock salt(AO) and perovskite(ABO_3) along the c-axis. The indirect exchange interaction of B-O-B takes place between the magnetic B ions in the perovskite layer.[3,4] The interlayer exchange interaction of B-O-O-B is weaker due to the larger distance between two neighboring magnetic ions as nearly twice the intraplanar distance and to also the geometry of which the molecular field in accordance with B-O-O-B interaction cancels out. Thus the oxides with K_2NiF_4 structure show 2 dimensional properties. The interaction of B ions in the perovskite layer mainly affects the physical properties of the oxides with K_2NiF_4 -type structure.

In A_2BO_4, the A ion can be replaced by the A′ ion with different size and charge, which may induce the mixed valence state of B ion, oxygen vacancy, and structural distortion.[5,6] Electrical conductivities and magnetic properties of the K_2NiF_4-type oxides have been investigated by many researchers[7~10] on the basis of ionic radii of A and B ions, the oxidation state and covalency of B ion, and the distribution of oxygen vacancies. Takeda[11,12] has studied the $Nd_{2-x}Sr_xNiO_4$ system in which conductivity increases with x value and is metallic above the x=0.60. An explanation has been proposed that the decreasing c/a ratio with increasing x value induces that the localized electron of d_{z^2}[1] orbital tends to populate the σ^* band formed by $d_{x^2-y^2}$ orbitals.

The interaction of B cations in the perovskite-type oxides is described by the superexchange model.[13,14] There are an antiferromagnetic interactions between the same Co^{3+} ions and also the same Co^{IV} ions, a ferrimagnetic interaction between Co^{3+} and Co^{IV} ions through σ and π bonds with O^{2-} ion, respectively, and a ferromagnetic interaction between Co^{3+} and Co^{IV} ions through σ bond with O^{2-} ion. If ionic radius of A ion is small in the K_2NiF_4 -type structure, the interaction of B ions can occur along c-axis. For example, in the $CaLa_{1-x}Y_xCrO_4$ system, Berjoan[15] has reported structural change and three dimensional(3D) interaction due to competing covalency of Cr-O and Y-O bonds with increasing x value.

Yang[16] has investigated the $(Gd_{1-x}Sr_x)_2CuO_4$ system of which Néel temperature remains unchanged below the composition of x=0.30 and decreases in the range from x=0.30 to 1.00. It is interpreted that the compositions of $0.00 \le x \le 0.30$ have T phase and the oxygen vacancies due to the Sr^{2+} ion doping are distributed along c-axis in the perovskite layer. Therefore Cu-O-Cu exchange interaction in the above compositions is retained. However the compositions of $0.30 < x \le 1.00$ have T′ phase in which the apical oxygen does not exist and thus oxygen vacancy is doped into the $Cu-O_2$ plane of the perovskite layer with decreasing Cu-O-Cu exchange interaction.

In the present study, solid solutions of the $Nd_{1-x}(Ba_{0.40}Mg_{0.60})_{1+x}FeO_{4-y}$($x$=0.00, 0.10, 0.20, and 0.30) system have been prepared. The crystallographic structure and the mixed valence state of Fe ion are analyzed by the x-ray powder diffraction analysis and Mohr salt titration, respectively. The magnetic susceptibility and electrical conductivity of the system have been measured and discussed with the variation of lattice parameters, the mixed valence state of Fe ion, the distribution of oxygen vacancies, and nonstoichiometric chemical formulas.

Experimental

Polycrystalline materials of the $Nd_{1-x}(Ba_{0.40}Mg_{0.60})_{1+x}FeO_{4-y}$ (x=0.00, 0.10, 0.20, and 0.30) system have been prepared by the ceramic method. Spectroscopic pure $BaCO_3$, $MgCO_3$, Fe_2O_3, and Nd_2O_3 powders are mixed and fired at 800 ℃ in air for 6 hours. After being well ground, the mixtures were heated at 1450 ℃ under an ambient atmosphere for

Table 1. Lattice parameters, unit cell volume, and crystal system for the $Nd_{1-x}(Ba_{0.40}Mg_{0.60})_{1+x}FeO_{4-y}$ system

x value	Lattice parameters (Å)			Unit cell	Crystal
	a	b	c	volume (Å^3)	system
0.00	11.342	11.848	12.369	1662.15	orthorhombic
0.10	11.362	11.856	12.391	1669.17	orthorhombic
0.20	11.350	11.856	12.392	1667.54	orthorhombic
0.30	11.345	11.851	12.402	1667.44	orthorhombic

Table 2. x, τ, y values, and nonstoichiometric chemical formula for the $Nd_{1-x}(Ba_{0.40}Mg_{0.60})_{1+x}FeO_{4-y}$ system

x value	τ value	y value	Nonstoichiometric chemical formula
0.00	0.04	−0.02	$Nd(Ba_{0.40}Mg_{0.60})Fe^{3+}_{0.96}Fe^{4+}_{0.04}O_{4.02}$
0.10	0.09	0.01	$Nd_{0.90}(Ba_{0.40}Mg_{0.60})_{1.10}Fe^{3+}_{0.91}Fe^{4+}_{0.09}O_{3.99}$
0.20	0.15	0.03	$Nd_{0.80}(Ba_{0.40}Mg_{0.60})_{1.20}Fe^{3+}{}_{0.85}Fe^{4+}{}_{0.15}O_{3.97}$
0.30	0.25	0.03	$Nd_{0.70}(Ba_{0.40}Mg_{0.60})_{1.30}Fe^{3+}{}_{0.76}Fe^{4+}{}_{0.24}O_{3.97}$

36 hours and then quenched. The grinding and heating processes were repeated several times in order to produce the homogeneous solid solution.

The crystallographic analysis has been carried out by the x-ray powder diffraction method with a PHILIPS pw 1710 diffractometer using monochromatized Cu Kα (λ=1.5406 Å) radiation. Lattice parameters, unit cell volume, and crystal system were determined reasonably.

The mixed valence state of Fe ion was analyzed by Mohr salt titration and the oxygen nonstoichiometricity of the solid solutions was calculated from the analysis according to electroneutrality condition.

Magnetic susceptibility was measured with DSM-8 magnetometer in the temperature range from 300 to 800 K. Magnetic parameters such as Curie constant and paramagnetic Curie temperature and effective magnetic moment of Fe ion were determined. Electrical conductivity of the pressed and sintered pellets was also measured by using four probe d.c. technique in the temperature range of 200-900 K under an ambient atmosphere.

Results and Discussion

The x-ray powder diffraction patterns of all the compositions are indexed on the basis of an orthorhombic phase having distorted K_2NiF_4 structures. The lattice parameters (σ_{max}=0.0012), unit cell volume, and crystal system in accordance with x value are shown in Table 1. The lattice parameters of a and b values are maximum at the x=0.10 and decrease in the compositional range from x=0.10 to x=0.30. The parameter of c value increases with the x value. Solid solutions for compositions of higher x values than 0.30 are not able to be synthesized.

The mole ratio of Fe^{4+} ion to the total Fe ion or τ value is determined by Mohr salt titration and the amount of oxygen vacancy or y value can be calculated by using the equation of $y=(x-\tau)/2$. The nonstoichiometric chemical formulas of all the compositions are listed in Table 2. The τ value

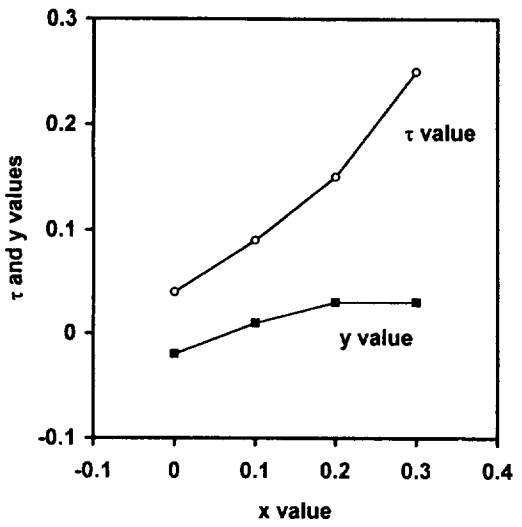

Figure 1. Plots of τ and y values *vs.* x value for the $Nd_{1-x}(Ba_{0.40}Mg_{0.60})_{1+x}FeO_{4-y}$ system.

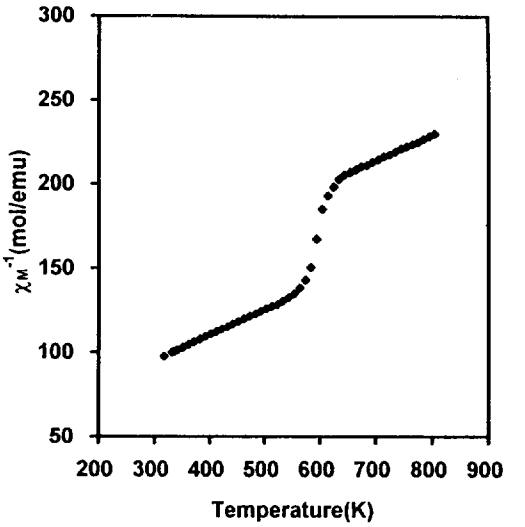

Figure 2. Plot of χ_M^{-1} *vs.* temperature for the $Nd(Ba_{0.40}Mg_{0.60})FeO_{4.02}$ system.

increases with x value as shown in Figure 1. The y value increases in the compositional range of $0.00 \le x \le 0.20$ and retains constant in the compositions of x=0.20 and 0.30. The variation of lattice parameters with x value in the $Nd_{1-x}(Ba_{0.40}Mg_{0.60})_{1+x}Fe^{3+}{}_{1-\tau}Fe^{4+}{}_{\tau}O_{4-y}$ system depends on the ionic radius of Nd^{3+} ion and average ionic radius of $(Ba_{0.40}Mg_{0.60})^{2+}$ ion, the mixed valence state and spin state of Fe ion, and the oxygen vacancy. From the small difference between radius of Nd^{3+} ion (r=130.3 pm) and average radius of $[Ba_{0.40}Mg_{0.60}]^{2+}$ ion (r=130.4 pm), the variation of a and b values depends on the mixed valence state and spin state of Fe ion. The variation of c value with x one is ascribed to the apical oxygen deficiency along the c-axis in the perovskite layer which results in strong repulsion between Fe and $[Ba_{0.40}Mg_{0.60}]^{2+}$ ions.

The plots of reciprocal magnetic susceptibility *vs.* temperature for all the compositions are shown in Figures 2-5. Diamagnetic contribution of every ions to χ_M was corrected ac-

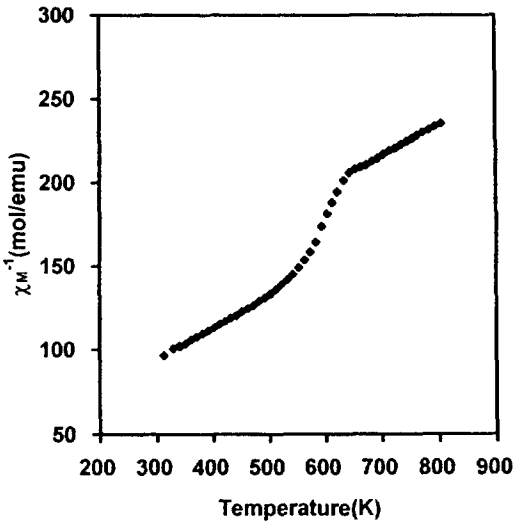

Figure 3. Plot of χ_M^{-1} *vs.* temperature for the $Nd_{0.90}(Ba_{0.40}Mg_{0.60})_{1.10}FeO_{3.99}$ system.

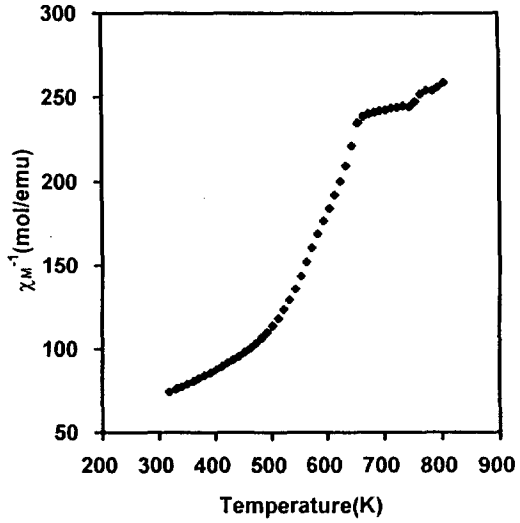

Figure 4. Plot of χ_M^{-1} *vs.* temperature for the $Nd_{0.80}(Ba_{0.40}Mg_{0.60})_{1.20}FeO_{3.97}$ system.

cording to Selwood.[17] Magnetic parameters such as the Curie constant (C) and the paramagnetic Curie temperature (θ_p) and effective magnetic moments (μ_{eff}) of Fe ions are listed in Table 3.

The negative paramagnetic Curie temperatures in all the compositions stand for antiferromagnetic interaction between Fe ions below the critical temperature, T_C. The interaction is ascribed to a canted antiferromagnetic one due to the distortion of FeO_6 sublattice in the perovskite layer and probably a ferrimagnetic one due to the superexchange one of Fe^{3+}-O^{2-}-Fe^{4+}. As shown in Figures 2-5, the critical temperatures remain unchanged despite of the increasing x value, which is similar to that observed in the $(Gd_{1-x}Sr_x)_2CuO_4$ system.[16] It seems that the increasing $(Ba_{0.40}Mg_{0.60})^{2+}$ ion does not affect the covalency of Fe and O^{2-} ions due to similar ionic radii of Nd^{3+} and $(Ba_{0.40}Mg_{0.60})^{2+}$ ions. Also oxygen vacancies do not weaken the exchange interaction of Fe ions, which means that oxygen vacancies are distributed not in

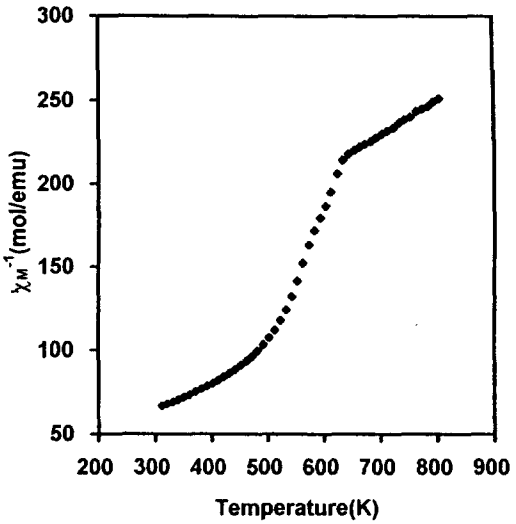

Figure 5. Plot of χ_M^{-1} *vs.* temperature for the $Nd_{0.70}(Ba_{0.40}Mg_{0.60})_{1.30}FeO_{3.99}$ system.

Table 3. Magnetic parameters and effective magnetic moments for the $Nd_{1-x}(Ba_{0.40}Mg_{0.60})_{1+x}FeO_{4-y}$ system

x value	Temperature range (K)	C	θ_p	$\mu_{eff(Fe)}$
0.00	632≤T≤804	6.59	−709.78	6.29
0.10	638≤T≤805	5.26	−437.19	5.50
0.20	734≤T≤804	4.79	−435.83	5.28
0.30	693≤T≤804	4.73	−370.38	5.31

the Fe-O_2 plane but along the c-axis of perovskite layer.

There are two regions with the different slopes of plots of the χ_M^{-1} *vs.* T in the paramagnetic region. In the upper region the total effective magnetic moment [μ_{eff}(total)] can be obtained by Curie-Weiss law. The exchange interaction between Nd^{3+} and Fe ions does not occur in the above region. Therefore the effective magnetic moment [μ_{eff}(Fe)] of Fe ion-only is calculated in each composition by using the equations of $\mu_{eff}^2(\text{total}) = \mu_{eff}^2(Nd^{3+}) + \mu_{eff}^2(Fe)$ and $\mu_{eff}(Nd^{3+}) = 3.62$ B.M. In the $Nd_{1-x}(Ba_{0.40}Mg_{0.60})_{1+x}FeO_{4-y}$ system, the mixed valence states of Fe^{3+} and Fe^{4+} ions are listed in Table 2.

The electrical conductivity measurements have been carried out in the temperature range from 200 to 900K under the atmospheric air pressure as shown in Figure 6. The activation energy of the conductivity obtained from the Arrhenius plots of electrical conductivities is listed in Table 4. For all the compositions, the conductivity increases with increasing temperature as a typical semiconductor behavior. The conductivity and activation energy as shown in Figures 6 and 7 do not depend on oxygen vacancy and $(Ba_{0.40}Mg_{0.60})^{2+}$ ion doping but only on the Fe^{4+} ion concentration. It shows that oxygen vacancies are formed along the c-axis in the perovskite layer and then can not impede the flow of electrons as a potential trapping site.

The e_g orbitals of iron ions overlap the p orbital of oxygen ion in the arrangement of Fe^{3+}-O^{2-}-Fe^{4+}. The e_g electron

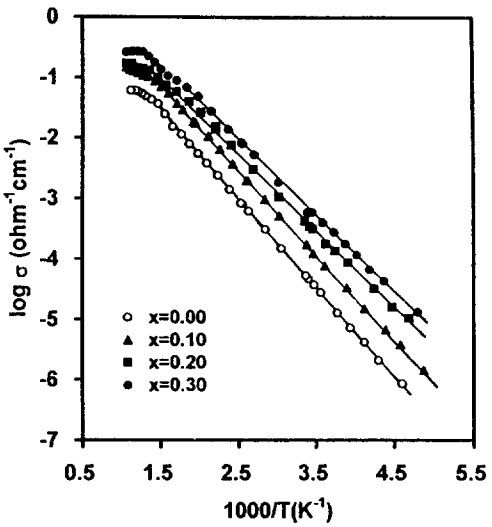

Figure 6. Plots of log σ *vs.* 1000/T for the $Nd_{1-x}(Ba_{0.40}Mg_{0.60})_{1+x}FeO_{4-y}$ system.

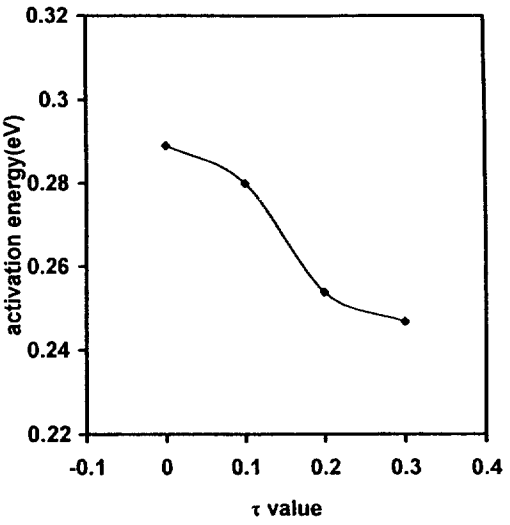

Figure 7. Plot of the activation energy *vs.* τ value for the $Nd_{1-x}(Ba_{0.40}Mg_{0.60})_{1+x}FeO_{4-y}$ system.

Table 4. Activation energy for the $Nd_{1-x}(Ba_{0.40}Mg_{0.60})_{1+x}FeO_{4-y}$ system

x value	Activation energy (eV)
0.00	0.289
0.10	0.280
0.20	0.254
0.30	0.247

transfer from Fe^{3+} ion into the vacant e_g orbital of Fe^{4+} ion through the bonds might be favorable, which means the hopping conduction mechanism. Therefore the conductivity and activation energy with increasing τ value increase and decrease, respectively, according to the conduction mechanism.

Conclusion

Oxygen vacancies doped with the increasing x value in the $Nd_{1-x}(Ba_{0.40}Mg_{0.60})_{1+x}Fe^{3+}{}_{1-\tau}Fe^{4+}{}_{\tau}O_{4-y}$ system are distributed along c-axis in the perovskite layer. Thus the oxygen vacancies do not affect the exchange interaction of Fe ions in perovskite layer. It results in that magnetic properties and electrical conductivity depend only on the mixed valence state of Fe ion. The canted antiferromagnetic and ferrimagnetic interactions between Fe ions coexist in the system and magnetic ordering temperature remains unchanged with x value. Electrical conductivity can be explained by the hopping of electron between e_g orbitals of Fe^{3+} and Fe^{4+} ions through the Fe^{3+}-O-Fe^{4+} bonds.

Acknowledgment. This work was supported by Grant No. 92-25-00-02 from the Korea Science and Engineering Foundation in 1993 and therefore we express our appreciation to the authorities concerned.

References

1. Hang, H. Y.; Cheong, S. W.; Copper, A. S.; Rupp Jr, L. W.; Batlogg, B.; Kwei, G. H.; Tan, Z. *Physica C* **1992**, *192*, 362.
2. Ganguly, P.; Rao, C. N. R. *J. Solid State Chem.* **1984**, *53*, 193.
3. Ganguly, P.; Rao, C. N. R. *Mat. Res. Bull.* **1973**, *8*, 405.
4. Flem, L. G.; Courbin, P.; Delmas, C.; Soubeyroux, J. L. *Z. Anorg. Alleg. Chem.* **1981**, *476*, 69.
5. Yo, C. H.; Kim, H. R.; Ryu, K. R.; Roh, K. S.; Choy, J. H. *Bull. Kor. Chem. Soc.* **1994**, *15*(8), 636.
6. Roh, K. S.; Ryu, K. S.; Ryu, K. H.; Yo, C. H. *Bull. Kor. Chem. Soc.* **1994**, *15*(7), 541.
7. Oh-Ishi, K.; Syono, Y. *J. Solid State Chem.* **1991**, 95, 136.
8. Chen, B. H.; Eichhorn, B. W. *J. Solid State Chem.* **1992**, *97*, 340.
9. Yokokawa, H.; Kawada, T.; Dokita. M. *J. Am. Ceram. Soc.* **1989**, *71*(1), 152.
10. Rao, C. N. R.; Ganguly, P.; Singh, K. K.; Ram, R. A. M. *J. Solid State Chem.* **1988**, *72*, 14.
11. Takeda, Y.; Nishijima, M. Imanishi, N.; Kanno, M.; Yamamoto, O.; Takano, M. *J. Solid State Chem.* **1992**, *96*, 72.
12. Goodenough, J. B.; Ramasesha, S. *Mat. Res. Bull.* **1982**, *17*, 383.
13. Ganaguly, P.; Kollali, S.; Rao, C. N. R.; Kern, S. *Magn. Lett.* **1980**, *1*, 107.
14. Day, P. *Acc. Chem. Res.* **1973**, *12*, 236.
15. Berkoan, R.; Coutures, J. P.; Flem, G. L.; Saux, M. *J. Solid State Chem.* **1982**, *42*, 75.
16. Yang, H. D.; Meen, T. H.; Chen, Y. C. *Physica C*, **1993**, *209*, 573.
17. Selwood, P. W. Magnetochemistry, 2nd ed, chap 5, Interscience, New York, 1967.